Key experimental information on intermediate-range atomic structures in amorphous Ge2Sb2Te5 phase change material

Shinya Hosokawa, Wolf-Christian Pilgrim, Astrid Höhle, Daniel Szubrin, Nathalie Boudet, Jean-François Bérar, and Kenji Maruyama

Citation: Journal of Applied Physics **111**, 083517 (2012); doi: 10.1063/1.3703570
View online: http://dx.doi.org/10.1063/1.3703570
View Table of Contents: http://scitation.aip.org/content/aip/journal/jap/111/8?ver=pdfcov
Published by the AIP Publishing

Key experimental information on intermediate-range atomic structures in amorphous $Ge_2Sb_2Te_5$ phase change material

Shinya Hosokawa,[1,2,a)] Wolf-Christian Pilgrim,[2] Astrid Höhle,[2] Daniel Szubrin,[2] Nathalie Boudet,[3] Jean-François Bérar,[3] and Kenji Maruyama[4]
[1]*Center for Materials Research Using Third-Generation Synchrotron Radiation Facilities, Hiroshima Institute of Technology, Hiroshima 731-5193, Japan*
[2]*Fachbereich Chemie, Physikalische Chemie, Philipps-Universität Marburg, Marburg 35032, Germany*
[3]*Institut Néel, Centre National de la Recherche Scientifique/Université Joseph Fourier (CNRS/UJF), Grenoble cedex 9 38042, France*
[4]*Department of Chemistry, Faculty of Science, Niigata University, Niigata 950-2181, Japan*

(Received 13 December 2011; accepted 13 March 2012; published online 19 April 2012)

Laser-induced crystalline-amorphous phase change of Ge-Sb-Te alloys is the key mechanism enabling the fast and stable writing/erasing processes in rewritable optical storage devices, such as digital versatile disk (DVD) or blu-ray disk. Although the structural information in the amorphous phase is essential for clarifying this fast process, as well as long lasting stabilities of both the phases, experimental works were mostly limited to the short-range order by x ray absorption fine structure. Here we show both the short and intermediate-range atomic structures of amorphous DVD material, $Ge_2Sb_2Te_5$ (GST), investigated by a combination of anomalous x ray scattering and reverse Monte Carlo modeling. From the obtained atomic configurations of amorphous GST, we have found that the Sb atoms and half of the Ge atoms play roles in the fast phase change process of order-disorder transition, while the remaining Ge atoms act for the proper activation energy of barriers between the amorphous and crystalline phases. © *2012 American Institute of Physics*. [http://dx.doi.org/10.1063/1.3703570]

I. INTRODUCTION

Rewritable optical storage devices, like digital versatile disk-random access memory (DVD-RAM) or blu-ray have meanwhile become common media for data storage and are widely used in all areas of daily life. The writing/erasing process on these devices is attained by a reversible laser-induced crystalline-amorphous transition of so-called phase change materials, such as $Ge_2Sb_2Te_5$ (GST). The transition occurs on a time scale of a few nanoseconds and is accompanied by a significant change of the optical and electrical properties. On the other hand, both of the phases must be sufficiently stable for more than ten years at ambient conditions. These properties are an excellent basis for the reversible data storage ability. However, the underlying microscopic processes enabling the above partly contradicting properties are not well understood yet. The important step toward an understanding of the mechanism is a detailed knowledge of the atomic structure participating in the phase transition.

The atomic structure of crystalline GST film is relatively well understood by x ray powder diffraction experiment;[1] it does not exhibit the stable crystal structure of hexagonal in ambient conditions, but a metastable rock salt structure, with Te atoms occupying sites on one face-centered-cubic (*fcc*) sublattice and with Ge, Sb, and 20% of vacancies forming another *fcc* sublattice. Convincing evidence for pronounced lattice distortions has been found in an x ray absorption fine structure (XAFS) experiment by Kolobov *et al.*,[2] where six Ge-Te neighboring bonds of the octahedral symmetry sites of the rock salt structure separate into three shorter and three longer bonds, as in GeTe crystal.[3]

The amorphous phase has also been explored with XAFS by Kolobov *et al.*,[2] who found remarkable decreases of Ge–Te and Sb–Te covalent bond lengths from those in the crystal. The data also indicated a change in the coordination number around Ge from sixfold in the crystal to fourfold in the amorphous. This observation, in combination with the aforementioned crystal lattice distortions, led the authors to propose an umbrella flip model for the fast phase transition, where the Ge atoms flip from an octahedral arrangement in the crystal to a tetrahedral environment in the amorphous phase. Another XAFS study[4] gave a different local structure around the Ge atoms that a significant concentration of the Ge–Ge wrong bonds exists in addition to the usual Ge–Te bonds. In addition, the environment around the Sb atoms was discussed to be mainly threefold-coordinated by Te atoms, like the distorted rock salt crystal.

Kohara *et al.*[5] measured the total structure factor, $S(Q)$, of the amorphous phase using high energy x ray diffraction and analyzed the data using a reverse Monte Carlo (RMC) calculation. Since GST is a three-component system, six partial correlation functions are, in principle, needed to fully describe the atomic arrangement. Using only a single $S(Q)$, they had to exclude the possibilities of cation–cation and Te–Te wrong bonds from the RMC calculation. As a result, these constraints force the amorphous phase to consist of even-membered ring structure only. Therefore, their conclusion that the resemblance of the even-membered ring structure is related to the fast phase change process is ambiguous.

[a)]Author to whom correspondence should be addressed. Present address: Department of Physics, Graduate School of Science and Technology, Kumamoto University, Kumamoto 860-0970, Japan. Electronic mail: hosokawa@sci.kumamoto-u.ac.jp.

By combining x ray and neutron total scattering results with XAFS data, Jóvári *et al.*[6] performed a RMC analysis. Thus, the reliability of the RMC output may be improved. However, the XAFS data do not help for investigating intermediate-range structures of amorphous GST, because information on amorphous structure from XAFS is mostly limited to the nearest neighboring atoms.

Instead of such a slow progress of the experimental studies, intermediate-range structural information has so far been obtained from theoretical works. Molecular dynamics (MD) calculations with density functional theory (DFT) were performed by Akola and Jones,[7] which shows a high degree of alternating four-membered rings (*ABAB* squares) being the main building blocks for the metastable rock salt crystal. An *ab initio* MD simulation was performed by Hegedüs and Ellott,[8] who also found very high densities of connected square rings. These fragments of the crystal were considered to be the origin of the fast phase-change process. Although it has not yet been explicitly stated, it is often implied in discussions of simulated results that the umbrella flip model is likely to be incorrect. On the other hand, the similarities of the local structures in the amorphous and crystalline phases intuitively indicate less stabilities of the phases, which contradicts the actual properties of the DVD media of long lasting phases.

As mentioned above, the key experimental information on the intermediate-range atomic structure in the amorphous phase is still lacking at present. In order to investigate the local and intermediate range order in the amorphous GST, an anomalous x ray scattering (AXS) experiment was carried out at energies close to the Ge, Sb, and Te *K* edges. With three sets of differential structure factors, $\Delta_i S(Q)$, together with total $S(Q)$, we have performed the RMC analysis. As already mentioned above, the reliability of RMC strongly depends on number and quality of the experimental scattering spectra. From the obtained atomic configurations of amorphous GST, we show that the environment around the Sb atoms indicates mostly the octahedral sites, as in the crystal phase, while that around the Ge atoms indicates both the octahedral and tetrahedral features. Four-membered rings of mainly Ge–Te–Ge–Te are observed with *puckered* shapes, which may be related to the difference of the electronic structures between the phases.

In this article, the experimental procedure and the data analysis are given in Secs. II and III, respectively. Results of experiment and RMC modeling are presented in Sec. IV. In Sec. V, we discuss the partial structure of amorphous GST with several structural parameters and 3D atomic configurations and present a plausible model suggested from the present structural data. A conclusion is given in Sec. VI.

II. EXPERIMENTAL PROCEDURE

The amorphous GST sample was prepared on a polycarbonate substrate in a sputter deposition device. The sample was scratched from the substrate and contained between two thin-walled ($\sim$50 μm) sapphire plates with a thickness of $\sim$50 μm for the Ge *K* edge experiment or in a quartz glass capillary with an inner diameter of 0.2 mm and a wall thickness of $\sim$10 μm for the Sb and Te *K* edges experiments.

The AXS technique utilizes the anomalous variation of the atomic form factor of a specific element near an x ray absorption edge of the respective element. The complex atomic form factor of an element is given as

$$f(Q,E) = f_0(Q) + f'(E) + if''(E), \tag{1}$$

where f_0 is the usual energy-independent term and f' and f'' are the real and imaginary parts of the anomalous term, respectively. When the incident x ray energy approaches an absorption edge of a constituent element, f' has a large negative minimum and f'' shows an abrupt jump.

One can utilize the difference between two scattering spectra near an absorption edge of the *i*th element $\Delta_i I$, where one is typically measured at some 10 eV and one at some 100 eV below the absorption edge (E_{near} and E_{far}, respectively). This differential intensity is expressed as

$$\alpha_i \Delta_i I(Q, E_{far}, E_{near}) = \Delta_i[\langle f^2\rangle - \langle f\rangle^2] + \Delta_i[\langle f\rangle^2]\Delta_i S(Q), \tag{2}$$

where α_i is a normalization constant and $\Delta_i[]$ indicates the difference of values in the bracket at the energies of E_{near} and E_{far} close to the absorption edge of the *i*th element.

The $\Delta_i S(Q)$ functions are given as a linear combination of partial structure factors $S_{ij}(Q)$ as

$$\Delta_i S(Q) = \sum_{i=1}^{N}\sum_{j=1}^{N} W_{ij}(Q, E_{far}, E_{near}) S_{ij}(Q). \tag{3}$$

Here, the weighting factors, W_{ij}, are given by

$$W_{ij}(Q, E_{far}, E_{near}) = x_i x_j \frac{\Delta_i[f_i f_j]}{\Delta_i[\langle f\rangle^2]}, \tag{4}$$

where x_i is the atomic concentration of *i*th element.

The AXS experiments were carried out using a standard $\omega - 2\theta$ diffractometer installed at the beamline BM02 of the European Synchrotron Radiation Facility (ESRF) in Grenoble, France. The scattering experiments were performed at two incident x ray energies below each *K* edge ($-$20 eV for Ge, $-$30 eV for Sb and Te, and $-$200 eV for all). For discriminating the elastic signal from the K_β fluorescence and Compton scattering contributions, a bent graphite crystal analyzer was mounted on a 50-cm-long detector arm. The feasibility of this setup is described elsewhere.[9–11]

III. DATA ANALYSIS

For the AXS data analysis, Sasaki's theoretical values[12] were used for the anomalous term and are given in Table I. The W_{ij} values were calculated with these f' and f'' values together with the theoretical $f_0(Q)$ values.[13] Following the procedure given in Ref. 14, $\Delta_i S(Q)$ spectra were calculated using Eqs. (1) and (2).

The W_{ij} values at $Q = 20\,\mathrm{nm}^{-1}$ near the first peak position in $S(Q)$ are tabulated in Table II. They slightly change with Q. As expected above, the edge-related $S_{ij}(Q)$ functions are enhanced and the other partials are highly suppressed.

TABLE I. The f' and f'' values in electron units at energies measured.

Element	Energy [eV]	f'_{Ge}	f''_{Ge}	f'_{Sb}	f''_{Sb}	f'_{Te}	f''_{Te}
Ge	10 904	**−3.651**	0.510	−0.198	3.524	−0.200	3.807
	11 084	**−5.982**	0.495	−0.211	3.427	−0.209	3.702
Sb	30 291	0.201	0.675	**−4.422**	0.571	−2.731	0.620
	30 461	0.199	0.668	**−6.029**	0.565	−2.858	0.614
Te	31 613	0.189	0.624	−2.701	3.344	**−4.480**	0.573
	31 783	0.187	0.617	−2.498	3.314	**−6.126**	0.567

RMC method[15] is a useful tool to construct three-dimensional (3D) structural models of disordered materials using experimental diffraction data. In the RMC simulation technique, the atoms of an initial configuration are moved so as to minimize the deviation from experimental structural data, e.g., in this study, $S(Q)$ and three differential structure factors, $\Delta_{Ge}S(Q)$, $\Delta_{Sb}S(Q)$, and $\Delta_{Te}S(Q)$, using a standard Metropolis Monte Carlo algorithm.[16]

The starting configuration of a system containing 13 500 atoms and the corresponding number density were generated using hard-sphere Monte Carlo simulations. In order to avoid unphysical atomic configurations, two constraints were applied: shortest atomic distances and bond angles. The choices of the shortest atomic distances were determined to avoid physically unreasonable spikes in $g_{ij}(r)$ in the low r range. The cut-off values were determined to be 0.23, 0.23, 0.20, 0.30, 0.20, and 0.30 nm for the Ge–Ge, Ge–Sb, Ge–Te, Sb–Sb, Sb–Te, and Te–Te atomic pairs, respectively. Weak bond angle constraints around the Te atoms were applied to be about 90°, which is based on the results of DFT calculation,[17] to keep the semiconducting nature of amorphous GST. The calculation box length was chosen to be 7.5395 nm, corresponding to the number density. The RMC simulations were performed using the RMC++ program package coded by Gereben *et al.*[18]

IV. RESULTS

Figure 1 shows $\Delta_i S(Q)$ obtained from the present AXS measurements close to the Ge (red circles), Sb (purple circles), and Te (blue circles) K edges, together with total $S(Q)$ given by black circles. These functions already indicate some interesting features. A small prepeak is observed in $S(Q)$ at about $Q = 10\,\mathrm{nm}^{-1}$, indicating the existence of an intermediate range atomic correlation. At this prepeak position, $\Delta_{Ge}S(Q)$ has a prominent peak, while $\Delta_{Sb}S(Q)$ and $\Delta_{Te}S(Q)$ show only small peaks similar in $S(Q)$. Thus, the intermediate-range correlations originate from the atomic

TABLE II. The W_{ij} values of $S_{ij}(Q)$ at $Q = 20\,\mathrm{nm}^{-1}$ near the first peak position in $S(Q)$.

Data	Ge–Ge	Ge–Sb	Ge–Te	Sb–Sb	Sb–Te	Te–Te
$S(Q)$	0.026	0.075	0.167	0.054	0.281	0.367
$\Delta_{Ge}S(Q)$	0.125	0.243	0.608	0.002	0.010	0.012
$\Delta_{Sb}S(Q)$	0.000	0.136	0.028	0.191	0.545	0.100
$\Delta_{Te}S(Q)$	0.000	−0.008	0.176	−0.013	0.232	0.613

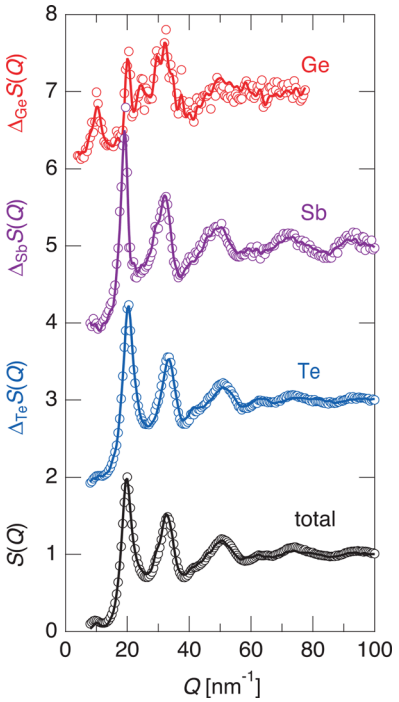

FIG. 1. $\Delta_i S(Q)$ obtained close to the Ge (red circles), Sb (purple circles), and Te (blue circles) K edges together with $S(Q)$ given by black circles. The solid curves indicate the best fits of the RMC modeling analysis. For clarity, the spectra are displaced upwards by 2.

correlations related to the Ge atoms. Also, $\Delta_{Ge}S(Q)$ provides only a small contribution to the distinct first maximum of $S(Q)$ at about $Q = 20\,\mathrm{nm}^{-1}$. On the other hand, these features are hardly seen in $\Delta_{Sb}S(Q)$ and $\Delta_{Te}S(Q)$, which are very similar to $S(Q)$. Thus, it is no doubt that the atomic arrangements around the Ge atoms are considerably different from the sites of the other constitutes in the amorphous phase.

A RMC modeling was applied to these AXS results to obtain the three-dimensional atomic configurations in the amorphous GST. Solid curves in Fig. 1 show the best fits of the RMC atomic modeling, which coincide very well with the experimental data.

Partial structure factors, $S_{ij}(Q)$, obtained from the present RMC analysis for the AXS data are given in Fig. 2. The features of Sb–Sb and Te–Te partials are basically similar to each other, indicating similar local environments around the Sb and Te atoms, as in the metastable rock salt crystal. On the other hand, as expected from $\Delta_{Ge}S(Q)$, the Ge–Te-related partials $S_{GeGe}(Q)$, $S_{GeTe}(Q)$, and $S_{TeTe}(Q)$ are very different from the other partials.

Also, it is interesting that these Ge–Te-related partials resemble well those of $GeSe_2$ glass:[11,19] 1) The Ge–Ge correlation shows a prominent prepeak, indicating the existence of intermediate-range order; 2) the Ge–chalcogen partial structure has a minimum at the first maximum in $S(Q)$. $GeSe_2$ is a typical chalcogenide glass, in which the coordination numbers follow the so-called $8 - N$ rule,[10,11,19] where N is the number of outer shell electrons, i.e., Ge and Se are four- and twofold-coordinated, respectively. Thus, the amorphous structure around the Ge atoms is expected to be very different from the three- or sixfold-coordinated crystal.

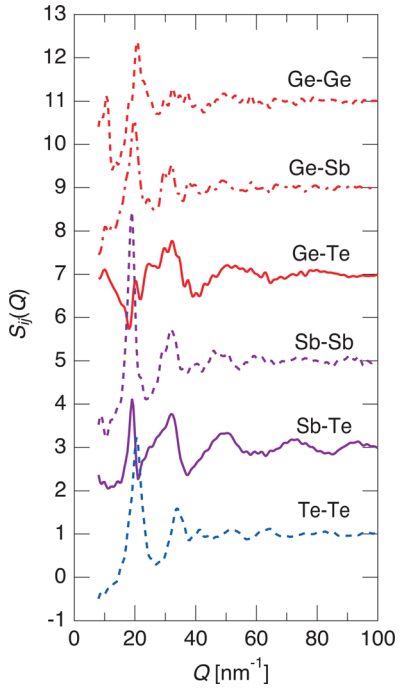

FIG. 2. The $S_{ij}(Q)$ spectra obtained from the RMC modeling. For clarity, the spectra are displaced upwards by 2.

Figure 3 shows partial pair distribution functions, $g_{ij}(r)$, obtained from the present RMC analysis. Overall features are similar to the results from the DFT calculation[17] and *ab initio* MD simulation.[20] The partial nearest neighbor distances obtained from $g_{ij}(r)$s are tabulated in Table III together with previous experimental and theoretical results.

Around the Ge atoms, the heteropolar Ge–Te bonds are seen in the $g_{\mathrm{GeTe}}(r)$ centered at $r = 0.265$ nm, in good agreement with the previous experimental results[2,4,6] and slightly

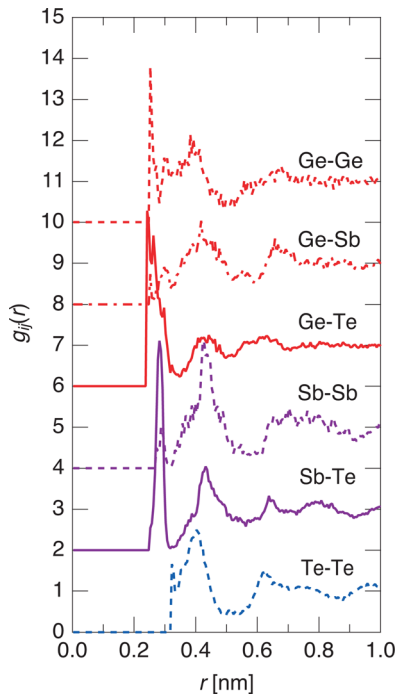

FIG. 3. The $g_{ij}(r)$ spectra obtained from the RMC modeling. For clarity, the spectra are displaced upwards by 2.

TABLE III. Partial nearest neighbor distances in nm.

	Ge–Te	Ge–Ge	Sb–Te	Ref.
Experiment				
AXS & RMC	**0.265(5)**	**0.250(10)**	**0.282(5)**	**Present**
XAFS	0.261(1)		0.285(1)	[2]
XAFS	0.263(1)	0.247(3)	0.283(1)	[4]
XD·ND·XAFS & RMC	0.264(2)	0.248(2)	0.283(2)	[6]
Theory				
DFT	0.278		0.293	[7]
DFT·XD & RMC	0.275	0.245	0.285	[17]
Ab initio MD	0.270		0.282	[8]
Ab initio MD	0.279		0.294	[20]

shorter than theoretical data.[7,8,17,20] In addition to the normal Ge–Te bonds, *wrong* Ge–Ge homopolar bonds are seen at $r = 0.25$ nm, which is again in good agreement with the XAFS result by Baker *et al.*[4] and the previous diffraction plus XAFS with RMC study.[6] The existence of such Ge–Ge wrong bonds contradicts the assumption in the XD with RMC study by Kohara *et al.*,[5] while Akola *et al.* combined the DFT calculation with RMC and this XD result and allowed the wrong bonds,[17] resulting in the Ge–Ge bond length matched with the present result.

Around the Sb atoms, the Sb–Te heteropolar bonds are mainly coordinated and centered at $r = 0.282$ nm, longer than the Ge–Te distance, which is in good agreement with all of the previous studies[2,4,6] and most of the theoretical works.[8,17]

The average total coordination numbers around the ith atoms, $\langle N_i \rangle$, and the average partial coordination numbers of jth atoms around the ith atoms, $N_{i\text{-}j}$, were calculated from $g_{ij}(r)$s, and are listed in Table IV together with the previous experimental and theoretical results. They were defined as the numbers of atoms located within the first minimum of each $g_{ij}(r)$, i.e., $r < 0.32$ nm. The $\langle N_{\mathrm{Ge}} \rangle$ value is 4.24, almost following the $8 - N$ rule around the Ge atoms. However, about 0.70 is composed of the *wrong* Ge–Ge bonds. Therefore, the fourfold coordination around Ge in Kolobov's umbrella flip model[2] is correct, whereas the atomic configurations are not purely $GeTe_4$ tetrahedra, unlike they suggested.

The total coordination number around the Sb atoms is 2.95, almost following the $8 - N$ rule. This result is in good agreement with the other experimental data,[4–6] while the theories mostly overestimated.[7,17,20] Most of the Sb atoms are surrounded by Te atoms ($N_{\mathrm{Sb\text{-}Te}} = 2.51$), and the Sb–Ge and Sb–Sb bonds are slightly seen ($N_{\mathrm{Sb\text{-}Ge}} = 0.28$ and $N_{\mathrm{Sb\text{-}Sb}} = 0.16$).

The $N_{\mathrm{Te\text{-}Ge}}$ and $N_{\mathrm{Te\text{-}Sb}}$ values are, respectively, 1.30 and 1.00, and the average total coordination number, $\langle N_{\mathrm{Te}} \rangle$, is about 2.30, similar to most of the theoretical results,[7,17,20] but exceeding the $8 - N$ rule value of two, unlike the previous experimental study by Jóvári *et al.*[6] and the theoretical work by Hegedüs and Elliott.[8]

V. DISCUSSION

Bond angle distributions around the Ge atoms are the most controversial issue on the intermediate-range structure of

TABLE IV. Partial average coordination numbers.

	$\langle N_{Ge}\rangle$	N_{Ge-Te}	N_{Ge-Ge}	$\langle N_{Sb}\rangle$	N_{Sb-Te}	$\langle N_{Te}\rangle$	N_{Te-Ge}	N_{Te-Sb}	Ref.
Experiment									
AXS & RMC	**4.24**	**3.26**	**0.70**	**2.95**	**2.51**	**2.30**	**1.30**	**1.00**	**Present**
XAFS		3.3	0.6		2.8		1.2	1.2	[4]
XD & RMC	3.7			3.0					[5]
XD·ND·XAFS & RMC	4.24		0.69	3.22		2.04	1.08	0.96	[6]
Theory									
DFT	4.2		0.4	3.7		2.9			[7]
DFT·XD & RMC	3.92	3.35	0.36	3.41	2.65	2.56	1.33	1.06	[17]
Ab initio MD	~4			~3		~2			[8]
Ab initio MD	3.823	3.277	0.275	4.025	3.166	2.866	1.311	1.267	[20]

amorphous GST. Kolobov *et al.* proposed the umbrella flip model, in which the Ge atoms have tetrahedral configurations under precondition.[2] On the contrary, a single peak was observed at an angle only slightly larger than 90° in the XD/RMC by Kohara *et al.*[5] and the DFT by Akola and Jones.[7] From these results, they emphasized that a significant number of fragments of the octahedral rock salt metastable crystal are included in the amorphous GST, and this is the origin of the fast amorphous-crystal phase change. On the other hand, Akola and Jones also pointed out that the peak is broad and includes tetrahedral symmetry, which becomes prominent if the Ge–Te bonds are defined to be shorter. Furthermore, double peaks were presented by the *ab initio* MD result performed by Hegedüs and Elliott.[8] The dominant maximum around the Ge atoms at an average value of about 90° indicates that the coordination geometry of Ge atoms is predominantly locally octahedral in character, although tetrahedral configurations are also evident from the subsidiary peak at 109°. The octahedral:-tetrahedral ratio is about 1.0:0.7. Another *ab initio* MD result by Caravati *et al.*[20] also shows the existence of tetrahedral symmetry around the Ge atoms to be 33%.

Figure 4 shows the bond angle distributions around the Ge (red), Sb (purple), and Te (blue) atoms obtained from the present AXS study. Around the Ge atoms, the spectrum is widely distributed and seems to have two peaks: one centered at 90°, characteristic of ideal octahedral atomic configuration, and one centered at about 109°, suitable for ideal tetrahedral configuration. The portions of octahedral and tetrahedral symmetries are almost the same. On the other hand, the bond angle distributions around the Sb atoms show only a single peak at an angle slightly larger than 90°. This result is in good agreement with the previous experiments and theories cited above.

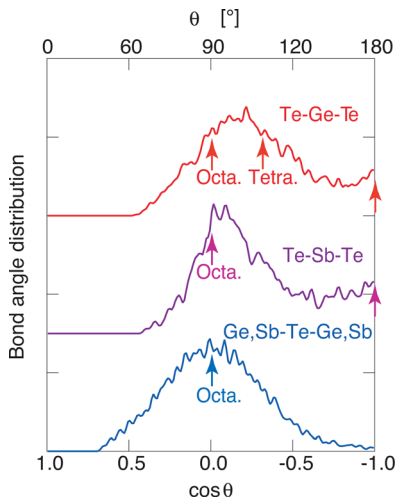

FIG. 4. Bond angle distributions around the Ge (red), Sb (purple), and Te (blue) atoms. Arrows show the angles of ideal tetrahedral, octahedral, and straight atomic configurations. For clarity, the spectra are displaced upwards.

Figure 5(a) shows the atomic configuration of Ge (red), Sb (purple), and Te (blue) atoms in amorphous GST obtained from the RMC modeling. From the same atomic configuration, tetrahedral or pyramidal units are deduced around the Ge and Sb atoms, which are, respectively, illustrated in Figs. 5(b) and 5(c). Around the Ge atoms, they are mainly tetrahedral units, and Ge–Te_4 and Ge–$GeTe_3$ tetrahedra coexist. Around the Sb atoms, on the other hand, they are mainly Sb–Te_3 pyramidal units together with a small portion of the T shape configurations, both of which are fragments of the rock salt crystal structure.

Figure 5(d) shows only the square rings extracted from Fig. 5(a). Square rings can be seen in amorphous GST, as pointed out by Akola and Jones[7] and Hegedüs and Elliott.[8] About 40% of the constituent atoms belong to these rings. Two interesting results are found from the present analysis. First, more than 50% of Ge atoms are the members of square rings, while only about 30% of Sb atoms form square rings. Thus, the square rings are preferably made up of Ge–Te–Ge–Te, which was not pointed out by the theories.[7,8] Second, the shapes of the square rings are mostly highly puckered, unlike the illustrations in Refs. 7 and 8. Thus, the square rings should be unpuckered on the amorphous-to-crystalline phase transition and vice versa.

Structurally, puckered or unpuckered square rings are topologically same. However, this slight structural change may largely affect the electronic structures. Huang and Robertson[21] pointed out that the optical matrix elements are enhanced in the crystal by aligned rows of resonantly bonded *p* orbitals, and due to the absence of this order, amorphous phases have normal-sized matrix elements. By the formation of puckered shapes of square rings on the crystalline-amorphous phase change, the *p* orbitals loose the directional order, which should induce significant changes of the electronic properties.

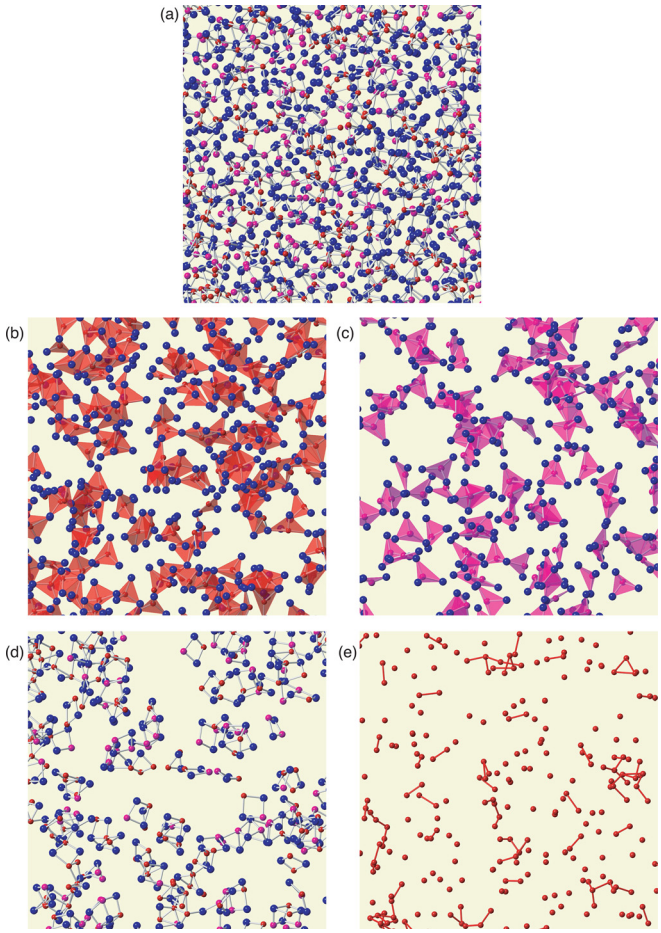

FIG. 5. (a) An example of atomic configuration of Ge (red), Sb (purple), and Te (blue) atoms. (b) Tetrahedral or pyramidal units around the Ge atoms. (c) Those around the Sb atoms. (d) Square rings made of mainly Ge–Te–Ge–Te with *puckered* shapes. (e) The Ge atoms with the wrong bonds given by bars.

Figure 5(e) shows only the Ge atoms (red balls) and the wrong Ge–Ge bonds (bars) extracted from Fig. 5(a). It is very interesting that a large number of chains of the Ge–Ge wrong bond are observed. These seem not to be induced by a simple mechanism that the fast amorphous-crystalline phase transition in GST originates from the similarity of the atomic fragments between two phases, in particular, around the Ge atoms. Instead, collective motions of the Ge atoms may be necessary on the phase transition.

Based on the present experimental results, we discuss a model for the phase change process in GST. As mentioned in the introductory section, the laser-induced amorphous-crystal phase change in GST should happen on a fast time scale of a few nanoseconds, while, once the phases are formed, these phases should be very stable for more than ten years at room temperature.

From structural points of view, the fast phase change is relatively easy to understand by considering the similarity of the local structures between the amorphous and crystalline phases, as discussed in previous experimental[5,17] and theoretical[8,17,21] papers.

Around the Sb atoms, it is very clear that the local environment in the amorphous phase remarkably resembles that in the crystal, as illustrated in Fig. 6. Namely, the Sb atoms

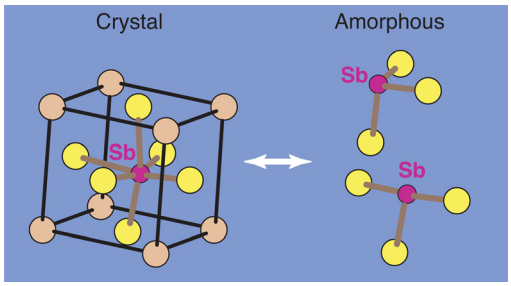

FIG. 6. Comparison between the crystalline and amorphous phases around the Sb atoms (Sb: small purple balls, Te: large balls with other colors).

are mostly threefold-coordinated with the Te atoms. The majority of the configurations are the pyramidal units with bond angles of ~90°, which is very similar to that in the distorted rock salt crystal, as shown in the figure. A small number of the T-shaped $SbTe_3$ are also building blocks of the distorted rock salt crystal. Therefore, no further story would be necessary for the local environments around the Sb atoms.

About half of Ge atoms have octahedral symmetry, as shown in the bond angle distributions in Fig. 4, and thus, the above mechanism for the Sb atoms is also applicable to these Ge atoms. Different from the Sb atom case is that an additional Te or Ge neighboring atom should be connected with the central Ge atom.

Let us start from the crystal structure around Ge atom illustrated in Fig. 7(a). If the additional atom is Te, it is very easy to build a $GeTe_4$ block by dragging one of the Te atoms having a longer bond with the central Ge into the block, as illustrated in Fig. 7(b), in the amorphous phase. This model was already proposed by Huang and Robertson.[21] Therefore,

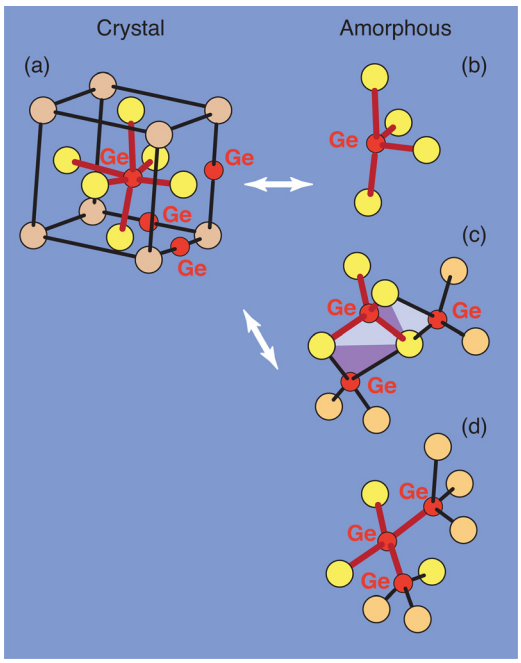

FIG. 7. Comparison between the crystalline and amorphous phases around the Ge atoms (Ge: small red balls, Te: large balls with other colors). Amorphous phase: (a) $GeTe_4$ with octahedral bond angles; (b) puckered Ge–Te–Ge–Te square rings; (c) Ge–Ge wrong bond chains.

all of the Sb atoms and half of the Ge atoms may contribute the fast phase change of GST.

If the additional atom is Ge, however, it is not easy to make a Ge–$GeTe_3$ block, because the neighboring Ge atom is located at the second nearest neighboring positions, indicated by red balls in the crystal structure in Fig. 7(a). To build a block by dragging the second neighboring Ge atom with a simple translational motion, a second neighboring Ge atom should push two of the nearest neighboring Te atoms away to make its own path to form the Ge–$GeTe_3$ block.

As regards another half of Ge atoms having the tetrahedral symmetry, this simply reflects the structural nature of Ge atoms that they prefer the tetrahedral symmetry rather than octahedral symmetry, due to the sp^3 hybridizations of the electrons if the structural constraints of the long-range order are lost on the amorphization. However, the fact that the portion of the tetrahedral symmetry around the Ge atoms is no more than a half indicates that intermediate-range constraints similar to the crystalline GST are still highly preserved in the amorphous phase.

The present AXS with RMC study gives other questions on the atomic configurations around the Ge atoms.

1) Why do the square rings prefer Ge–Te–Ge–Te configurations with puckered forms, as illustrated in Fig. 7(d)?
2) Why do the Ge–Ge wrong bonds tend to form the chains, as illustrated in Fig. 7(e)?

These problems cannot be easily solved by a simple translation motion of the atoms on the crystalline-amorphous phase transition. For example, two pyramidal $GeTe_3$ units in the crystal can be connected by forming a new Ge–Ge bond. However, this process only produces an ethane-like Te_3–Ge–Ge–Te_3 configuration and cannot make a further connection with a third $GeTe_3$ building block. Thus, a different scenario should be necessary.

The model that we suggest here from the present AXS with RMC work is a modified version of the umbrella flip model proposed by Kolobov *et al.*[2] We start from the distorted rock salt crystal, as shown in Fig. 8(a).

If the octahedral Ge atom at the center of the cubic crystal (the small red ball in Fig. 8(a)) flips through the white triangle to the tetrahedral symmetry, as shown by the small pink ball in Fig. 8(b), the flipped Ge atom can meet other Ge atoms at the three edges, as suggested by Kolobov *et al.*,[22] with a probability of 40% each. Suppose that there are two Ge atoms near the flipped Ge atom, as illustrated in Fig. 8(b), which is larger than the statistical result of 1.2, but still highly possible. If these two Ge atoms do not flip and make new covalent bonds with the flipped Ge atom, it can be very easy to form a wrong bond chain with three Ge atoms, as illustrated in Fig. 8(d).

Another story happens when the neighboring Ge atoms also flip from the original positions possessing two Te atoms with the previously flipped Ge atom. As shown in Fig. 8(c), edge-sharing $GeTe_4$ tetrahedra are formed. Note that such edge-sharing tetrahedra always have the puckered square rings, as depicted by the shadows in the figure.

From only the geometrical points of view, thus, it is highly plausible in the findings from the present AXS + RMC study that the wrong bond chains and the puckered square rings with Ge–Te–Ge–Te can be clearly explained by the above-modified and detailed flip motions of the Ge atoms on the crystalline-amorphous phase transition. In reality, however, the energy barrier of the flip motion is very important.

The energy barrier of the phase transition was experimentally obtained[23] and is a quite high value of about 2.4 eV for GST. Such a large barrier is necessary to give a long (10 years) storage lifetime at room temperature. A DFT calculation gave similar values of some eV for the umbrella flip motion.[24] Thus, it is suggested that the umbrella flip motion of the Ge atoms is not the key dynamic for the *fast* phase change process, unlike Kolobov *et al.*[2] proposed, but acts for the *long* lifetime as an optical storage at ambient conditions.

The most critical problem is, however, still unsolved, i.e., how the Ge atoms can flip over such a high energy barrier at high temperatures. Another disadvantage of this idea is the fact that the flip motions have not yet been reported by *ab initio* MD simulation works. Since the energy barrier calculated by the DFT was carried out by a simple movement of a Ge atom and the results highly depend on local environment around the Ge atoms in the crystalline phase,[24] it is possible that the cooperative and complex motions of Ge and Te atoms can lower the local energy barrier of the flip motions.

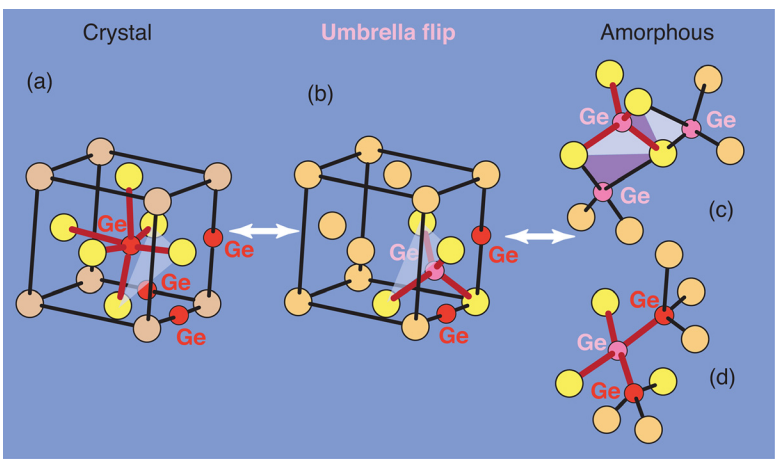

FIG. 8. A modified umbrella flip model based on the present AXS experiment with RMC. Large balls: Te; red small balls: unflipped Ge atoms; pink small balls: flipped Ge atoms.

Investigations on the structure of the liquid phase would also be important to understand the mechanism of the phase change, because the transition from the crystal to amorphous phases undergoes through the liquid phase. The total $S(Q)$ function of liquid GST was obtained by Kohara *et al.*[5] using XD, and the features of $S(Q)$ of the liquid phase seem to be similar to those of the amorphous phase, except damping. The result was analyzed again using RMC. Although the results of the liquid structure parameters are not presented in detail in their paper, the ring statistics in the liquid phase resembles that in the amorphous phase very well and is different from that in the crystal. Kolobov *et al.*[25] carried out XAFS measurements on liquid GST near the Ge, Sb, and Te *K* edges. Although difficulties, such as the determination of the coordination numbers, arise in the data analysis process, owing to the damped spectral features, the bond lengths of Ge–Te and Sb–Te are very similar to the amorphous values. Moreover, results of the x ray absorption near-edge structure (XANES), which contain information about the spatial arrangement of the neighbors around the absorbing elements, reveal that the XANES spectra of the liquid phase closely resemble those of the amorphous phase, but are very different from the crystal. From these experimental results, thus, they concluded that the local structures of liquid GST are very similar to those of amorphous GST, suggesting a semiconducting nature of the melt.

Akola and Jones performed DFT calculations also for the liquid phase,[26] which provide more detailed partial information about the liquid structures. Similar to the experimental results, the features of the total $S(Q)$ and $g(r)$ show no significant differences between the liquid and amorphous phases, except damping. In the partial $g_{ij}(r)$ functions, however, an interesting difference is observed, as shown in Fig. 3 and Table I of Ref. 26, i.e., the Ge–Ge and Ge–Sb homopolar partial coordination numbers increase quite largely on melting from the amorphous to liquid phases, while the Ge–Te and Sb–Te heteropolar coordinations decrease. On the other hand, the Sb–Sb homopolar coordination number remains unchanged on melting. From these results, homopolar bonds including the Ge atoms, are more favorable configurations in liquid GST than those in amorphous GST. Assuming that the liquid is the intermediate phase on the crystal-amorphous transition in the present modified umbrella flip model, the Ge–Ge and Ge–Sb nearest neighboring wrong bonds are easily formed, as seen in Fig. 8(b). (Some Ge atoms at the edges of the cubic cell can be replaced by Sb atoms.) Thus, the results of the DFT calculation may support the present model. In order to confirm such partial structures of liquid GST experimentally, AXS with RMC modeling is an excellent method, which is now in progress.

Finally, a different crystalline structure of GST proposed recently is introduced to consider the transition mechanism from a different point of view. From an x ray fluorescence holography (XFH) measurement on a single crystalline GST thin film with the rock salt structure, Ge atoms with tetrahedral symmetry were found in the 3D atomic image reconstructed from an XFH hologram.[27] This reveals that the amorphous-like tetrahedral symmetry is already prepared in the crystal phase. Although the single crystal GST measured is not identical to the real DVD material of polycrystalline form, this result indicates that the tetrahedral symmetry is energetically very near the octahedral symmetry of the rock salt crystal. Very recently, using electron microscopy and diffraction techniques as well as first principles calculations, about one-third of the Ge atoms in the cubic phase of GST were observed to be located in tetrahedral environments.[28] If these findings are true, the umbrella flip motion illustrated between Figs. 8(a) and 8(b) is no longer necessary. On the other hand, the origin of the long-lasting stabilities of the phases at room temperature discussed above would be lost.

These studies mentioned above are, however, limited to the static structures of this material, which is only a projected figure of the real processes. A further experiment for the dynamic properties, such as inelastic experiment, is essential to clarify the mechanism, such as to examine the existence of the flip motions, on the crystalline-amorphous phase change process in GST.

VI. CONCLUSION

In conclusion, the short and intermediate-range atomic structures of amorphous GST were investigated by a combination of AXS experiment and RMC modeling for clarifying the fast crystalline-amorphous phase change process and long lifetime as a storage material. From the obtained atomic configurations of amorphous GST, we have found that the Sb atoms and half of the Ge atoms have octahedral environments similar to those in the crystal, which may play roles in the fast phase change process. The remaining Ge atoms with the tetrahedral symmetry act for the proper energy barrier between the phases if umbrella flip motions happen. A large number of puckered square rings result in highly disordered *p* electron directions, inducing a significant reduction of the resonant bonds and optical matrix elements in the amorphous phase. These findings around the Ge atoms, as well as the formation of wrong Ge–Ge bond chains, can also be explained by a modified and detailed version of an umbrella flip motion of some Ge atoms on the order-disorder transition in GST.

ACKNOWLEDGMENTS

We acknowledge Professor M. Wuttig of Rheinisch-Westfälische Technische Hochschule Aachen for providing the amorphous GST samples. The AXS experiments were performed at the beamline BM02 of the ESRF (Proposal No. HD279, HD380, HD466, and HD510).

[1]N. Yamada and T. Matsunaga, J. Appl. Phys. **88**, 7020 (2000).
[2]A. V. Kolobov, P. Fons, A. I. Frenkel, A. L. Ankudinov, J. Tominaga, and T. Uruga, Nature Mater. **3**, 703 (2004).
[3]T. Chattopadhyay, J. X. Boucherle, and H. G. von Schnering, J. Phys. C **20**, 1431 (1987).
[4]D. A. Baker, M. A. Paesler, G. Lucovsky, S. C. Agarwal, and P. C. Taylor, Phys. Rev. Lett. **96**, 255501 (2006).
[5]S. Kohara, K. Kato, S. Kimura, H. Tanaka, T. Usuki, K. Suzuya, H. Tanaka, T. Matsunaga, N. Yamada, Y. Tanaka, H. Suematsu, and M. Takata, Appl. Phys. Lett. **89**, 201910 (2006).

[6]P. Jóvári, I. Kaban, J. Steiner, B. Beuneu, A. Schöp, and A. Webb, J. Phys.: Condens. Matter **19**, 335212 (2007).
[7]J. Akola and R. O. Jones, Phys. Rev. B **76**, 235201 (2007).
[8]J. Hegedüs and S. R. Elliott, Nature Mater. **7**, 399 (2008).
[9]S. Hosokawa and J.-F. Bérar, AIP Conf. Proc. **879**, 1743 (2007).
[10]S. Hosokawa, I. Oh, M. Sakurai, W.-C. Pilgrim, N. Boudet, J.-F. Bérar, and S. Kohara, Phys. Rev. B **84**, 014201 (2011).
[11]S. Hosokawa, W.-C. Pilgrim, J.-F. Bérar, and S. Kohara, Phys. Status Solidi A **208**, 2544 (2011).
[12]S. Sasaki, *KEK Report 1989* (Nat. Lab. High Energy Phys., Tsukuba, 1989), p. 1.
[13]*International Tables for X-ray Crystallographie*, 2nd ed., edited by C. H. MacGillavry and G. D. Rieck (Kynoch, Birmingham, 1968), Vol. III.
[14]S. Hosokawa, Y. Wang, J.-F. Bérar, J. Greif, W.-C. Pilgrim, and K. Murase, Z. Phys. Chem. **216**, 1219 (2002).
[15]R. L. McGreevy and L. Pusztai, Mol. Simul. **1**, 359 (1988).
[16]N. Metropolis, A. W. Rosenbluth, M. N. Rosenbluth, A. H. Teller, and E. Teller, J. Phys. Chem. **21**, 1087 (1953).
[17]J. Akola, R. O. Jones, S. Kohara, S. Kimura, K. Kobayashi, M. Takata, T. Matsunaga, R. Kojima, and N. Yamada, Phys. Rev. B **80**, 020201 (2009).
[18]O. Gereben, P. Jóvári, L. Temleitner, and L. Pusztai, J. Optoelectron. Adv. Mater. **9**, 3021 (2007).
[19]I. Petri, P. S. Salmon, and H. E. Fischer, Phys. Rev. Lett. **84**, 2413 (2000).
[20]S. Caravati, M. Bernasconi, T. D. Kühne, M. Krack, and M. Parrinello, Appl. Phys. Lett. **91**, 171906 (2007).
[21]B. Huang and J. Robertson, Phys. Rev. B **81**, 081204 (2010).
[22]A. V. Kolobov, P. Fons, and J. Tominaga, Phys. Status Solidi B **246**, 1826 (2009).
[23]J. Kalb, F. Spaepen, and M. Wuttig, Appl. Phys. Lett. **84**, 5240 (2004).
[24]C. Lang, S. A. Song, D. N. Manh, and D. J. H. Cockayne, Phys. Rev. B **76**, 054101 (2007).
[25]A. V. Kolobov, P. Fons, M. Krbal, R. E. Simpson, S. Hosokawa, T. Uruga, H. Tanida, and J. Tominaga, Appl. Phys. Lett. **95**, 241902 (2009).
[26]J. Akola and R. O. Jones, J. Phys.: Condens. Matter **20**, 465103 (2008).
[27]S. Hosokawa, T. Ozaki, K. Hayashi, N. Happo, M. Fujiwara, K. Horii, P. Fons, A. V. Kolobov, and J. Tominaga, Appl. Phys. Lett. **90**, 131913 (2007).
[28]X. Q. Liu, X. B. Li, L. Zhang, Y. Q. Cheng, Z. G. Yan, M. Xu, X. D. Han, S. B. Zhang, Z. Zhang, and E. Ma, Phys. Rev. Lett. **106**, 025501 (2011).